

# Positive effects of ferric iron on the systemic efficacy of nephrilin peptide in burn trauma

Desmond D Mascarenhas<sup>1,2</sup> , Amina El Ayadi<sup>3,4</sup>,  
Puja Ravikumar<sup>5</sup>, Gyeong Jin Kang<sup>5</sup>, Tammy Langer<sup>5</sup>,  
Carlos Moreno<sup>5</sup> and Edward P Amento<sup>5</sup>

## Abstract



**Introduction:** Nephrlin peptide is a designed inhibitor of Rictor complex (also known as mTORC2), an evolutionarily conserved assembly believed to modulate responses to cellular stress. We previously demonstrated the ability of nephrlin peptide to suppress neuroinflammation, loss of body mass, glycaemic control and kidney function in a rat scald model, as well as sepsis mortality in a mouse model. The present study explores the effect of nephrlin plus iron formulations on clinically relevant outcomes in the rat scald model.

**Methods:** Animals were treated with nephrlin by subcutaneous bolus injection on post-burn days 1–7. Equimolar ferric iron in the formulation improved the positive systemic effects of nephrlin on kidney function, glycaemic control, oxidative stress, early hyperinflammation, late inflammasome activation, hyperangiogenesis and body mass, all variables previously shown to bear upon clinically relevant burn injury outcomes. The sparing effects of nephrlin-iron were demonstrated in both sexes.

**Discussion:** Surprisingly, optimum daily treatment doses were in the range of 2–4 mg/kg, while 8 mg/kg was less effective, suggesting the possibility of marginal pro-oxidant effects from the ‘free’ iron fraction. Thus, although ferric iron in the nephrlin formulation is clearly helpful, care must be exercised to select an optimum treatment dose.

**Conclusion:** Iron increases the efficacy of nephrlin peptide in burns.

## Keywords

Nephrlin, trauma, burn injury, systemic, iron, hyperinflammation, kidney function, glycaemic control, pathological angiogenesis

<sup>1</sup>Mayflower Organization for Research & Education, Sunnyvale, CA, USA

<sup>2</sup>Transporin, Inc., Sunnyvale, CA, USA

<sup>3</sup>Department of Surgery, The University of Texas Medical Branch, Galveston, TX, USA

<sup>4</sup>Shriners Hospitals for Children - Galveston, Galveston, TX, USA

<sup>5</sup>Molecular Medicine Research Institute, Sunnyvale, CA, USA

## Corresponding author:

Desmond D Mascarenhas, Mayflower Organization for Research and Education, 428 Oakmead Pkwy, Sunnyvale, CA 94085, USA.

Email: [desmond@transporin.com](mailto:desmond@transporin.com)



## Lay Summary

Nephrilin peptide is a novel treatment for burn trauma. It addresses the serious and often long-lasting systemic effects of burn trauma on organ function, metabolism and the immune system. Trauma is often associated with anaemia. The present study asks whether the efficacy of nephrilin can be improved by the addition of iron. In a rat scald model, there is a significant improvement in outcomes when iron is added.

## Introduction

Mammalian target of rapamycin (mTOR) is a serine threonine kinase that exists in two physically and functionally distinct assemblies, Raptor complex and Rictor complex (also known as mTORC1 and mTORC2). These complexes share some components such as TOR kinase but differ in terms of their regulation and cellular functions, as well as their responsiveness to the allosteric inhibitor, rapamycin.<sup>1</sup> Rictor complex controls various members of the AGC sub-family of kinases, which includes Akt, serum and glucocorticoid-induced protein kinase 1 (SGK1), and protein kinases C-alpha and C-beta (PKC- $\alpha/\beta$ ). These kinases in turn regulate a range of cellular processes such as metabolism, survival, apoptosis, cytoskeletal architecture, cell motility, growth and proliferation by phosphorylating various effectors.<sup>2,3</sup> The peptide nephrilin is a designed inhibitor of Rictor complex that is actively transported into cells *in vivo*.<sup>4</sup> It binds to Rictor directly, preventing its binding to another component of the complex, Protor. Nephrilin was derived by fusing a 19 amino acid segment of Protor (a sequence common to the human, rat and mouse proteins) with the metal binding domain (MBD) of human insulin-like growth factor binding protein-3 (IGFBP3), a 21 amino acid sequence that targets and enters stressed cells.<sup>5,6</sup>

One of the reported activities of Rictor complex is super-activation of Rac1 (Ras-related C3 botulinum toxin substrate 1), a small GTPase and obligate subunit of activated NADPH oxidase, which plays a central role in oxidative metabolism in skin, kidney and other tissues. Rac1 controls several cellular processes, including generation of oxidative radicals and reorganisation of the actin cytoskeleton in both normal cell types and cancer cells.<sup>1,7</sup> The mechanism of action of nephrilin in rodent burn models appears to work through oxidative stress and Rac1 phosphorylation. Nephrilin treatment after burn injury reverses epigenetic and signalling

changes in kidney tissue that lead to the activation of Rac1, and lowers elevations in markers of oxidative stress such as urinary 8-isoprostane and plasma OHDG. By inhibiting a stress-responsive function of Rictor complex, nephrilin blocks the gratuitous upregulation of Rac1 caused by severe stress without affecting basal levels of Rac1 activation.<sup>8</sup> In theory, this represents a safer, more targeted intervention than, say, the use of TOR kinase inhibitors, whose effect upon house-keeping functions essential to cellular homeostasis are problematic.

Severe burn trauma is associated with a vast array of secondary effects including systemic inflammation, loss of lean body mass, sepsis, organ failure, loss of glycaemic control, delayed wound healing and cognitive deficits. These serious and enduring complications can lead to substantial morbidity and mortality.<sup>9–13</sup> We previously showed the pleiotropic effects of nephrilin peptide in combating post-burn systemic neuroinflammation, loss of glycaemic control, lean body mass and kidney function, and impaired wound healing in a rat scald model; and sepsis in a mouse model. Some, but not all, of these systemic effects of nephrilin appear to be influenced by the animal's iron status.<sup>14,15</sup> Severe trauma is associated with anaemia mediated by hepcidin, an iron-regulatory protein in serum and a current target of therapy in critical illness.<sup>16</sup>

In the present study, we use a well-established rat scald model<sup>17</sup> to explore the impact of a seven-day treatment regimen comprising subcutaneous bolus injection of nephrilin peptide with or without iron. The treatment begins after scald, in parallel with real-life injury. Nephrilin has previously been shown to modulate the neuroimmune response to a variety of xenobiotic and metabolic stressors in rodents.<sup>18,19</sup> When injected into mice at high doses daily for 26 days, nephrilin generates no visibly differential pathology compared to vehicle.<sup>18</sup> Nephrilin contains a metal-binding domain known to bind ferrous (Fe<sup>2+</sup>) and ferric (Fe<sup>3+</sup>) iron.<sup>6</sup> Based on cross-linking studies, uptake of this metal-binding

domain into mammalian cells involves binding to integrin-beta-3, a component of a major metal uptake pathway, and to transferrin receptor.<sup>19,20</sup>

## Material and methods

### Reagents

Nephrilin peptide, a 40-mer peptide carrying a sequence derived from PRR5/Protor (the sequence is conserved in human, rat and mouse species) was synthesised by Lifetein LLC (Hillsborough, NJ, USA) and purified to > 80% by high-performance liquid chromatography. The design and synthesis of nephrilin have been previously described.<sup>4</sup> Antibodies for ELISAs were purchased from Abcam (Cambridge, MA, USA) and chemicals from Sigma-Aldrich (St. Louis, MO, USA) unless otherwise specified.

### Nephrilin administration

Adult Sprague Dawley rats of both sexes (250–300 g, Charles River Laboratories, Wilmington, MA, USA) were injected with nephrilin peptide plus or minus equimolar metal (zinc, ferrous iron or ferric iron) once daily by subcutaneous bolus injection, days 1–7. Treatment group sizes were  $n = 8$  for each sex unless otherwise indicated: group S = sham-treated; group B = burn + vehicle; group N1 = burn + 4 mg/kg nephrilin; group N1/Zn2 = burn + 4 mg/kg nephrilin/zinc chloride; group N1/Fe2 = burn + 4 mg/kg nephrilin/ferrous sulphate; and groups N1/Fe3 (2, 4 or 8) = burn + 2, 4, or 8 mg/kg nephrilin/equimolar ferric chloride. The first dose was administered after completion of the scald procedure. Injection volume was 400  $\mu$ L. Control animals received the same volume of vehicle. The 4 mg/kg daily dosage of nephrilin was selected based on its demonstrated safety and efficacy in 11 different rodent disease models tested to date (unpublished data).<sup>7,10,11,14</sup> In a non-GLP study, mice that were treated daily with 20 mg/kg nephrilin by subcutaneous bolus for 26 days showed no differential toxicology in major organs when compared to a saline control.<sup>4</sup>

### Rat scald model

The rat scald burn model<sup>17</sup> is a modified Walker-Mason model that induces inflammation and hypermetabolism in line with what severely burned patients experience. The model results in a mortality rate of < 1%. Adult male Sprague Dawley rats were housed in clean cages on a 12-h light/dark cycle with access to food (standard

chow) and water ad libitum. Animals were allowed to acclimate for one week before the experiment. All animal procedures were performed in adherence to the National Institute of Health's *Guide for Care and Use of Laboratory Animals* and approved by the Institutional Animal Care and Use Committee (IACUC) of the Molecular Medicine Research Institute. All procedures were initiated in the morning between 07:00 h and 10:00 h. Prophylactic analgesia (0.05 mg/kg body weight Buprenorphin) was administered 15 min before general anaesthesia using isoflurane. The dorsum of the trunk and the abdomen were shaved, and a 60% of total body surface area (TBSA) burn administered by placing the animals in a mould and immersing them in water heated to 98–100 °C for 10 s on the back and 2 s on the abdomen, except that for anatomical reasons female rats received only the dorsal burn, thereby reducing the burn exposure for female rats. This method delivers a full-thickness cutaneous burn as confirmed by histological examination. Burned rats were immediately resuscitated with 40 cc/kg Ringer's Lactate injected intraperitoneally. Animals in the sham group were treated exactly as described above for burned animals except that the animals were placed in room temperature water. Animals were randomly assigned to treatment groups, and nephrilin (4 mg/kg) or saline were administered by subcutaneous bolus daily. Each treatment group comprised 16 animals (eight of each sex). At the end of the study period, animals were euthanised by decapitation as approved by MMRI IACUC guidelines, the NIH's Office of Laboratory Animal Welfare (OLAW) and AVMA recommendations. All tissues and organs of interest were rapidly dissected or collected and flash frozen in liquid nitrogen with subsequent storage at –80 °C.

### Glucose tolerance test

Fourteen days post-burn, the rat tail was snipped and the baseline glucose level measured using a BAYER contour blood glucose monitoring system. The rats were injected intraperitoneally with glucose and readings were performed at 30 min, 60 min and 120 min after injection. Results were expressed as areas under the curve (ug/dL/h) over baseline over the sampling period.

### Early hyperinflammation and inflammasome activation

Twenty-four hours after scald, a blood sample was taken from each (isoflurane anaesthetised) rat. Plasma IL-6 was measured using a rat IL-6 DuoSet

ELISA kit (R&D Systems, Minneapolis, MN, USA). Blood taken at 14 days post-burn was analysed for 27 cytokine and chemokine analytes including VEGF-A, IL-18, IL1-beta, CCL5 and CXCL5 (RD27 Custom Plex Discovery Assay, Eve Technologies, Calgary, AB, Canada).

### Plasma OHDG

Fourteen-day plasma was assayed for OHDG using an Oxidative Damage High Sensitivity ELISA Kit purchased from Cayman Chemical (Ann Arbor, MI, USA).

### Kidney function (plasma creatinine)

Kidney function was indirectly assessed by measuring 14-day plasma creatinine. Estimated glomerular filtration rate (eGFR; mL/min/100 g animal body weight) can be computed from this value as previously described.<sup>15,21</sup>

### PctRedPix computation

A digital image of each wound at two weeks post-scald were analysed using GIMP 2.10 software. Red pixels, as a percentage of all pixels within the wound area, were counted by the software and expressed as a percentage of total.

### Computation of efficacy

Aggregate efficacy of each treatment regimen was computed using an average of Z-scores calculated from the distribution of values for each analyte by subtracting the mean of the distribution from the value and dividing by the standard deviation for the distribution.

### Statistical analysis

Data are presented as means  $\pm$  SD unless otherwise indicated. *P* values were computed using Student's *t*-test and expressed relative to sham or saline-treated group.

## Results

Traditionally, in this model, male rats have been used. To our knowledge, the absence of published data on female rats reflects the possible confounding effects of oestrous cycles, as well as anatomical differences necessitating changes in scald procedure (see 'Materials and methods'). We therefore tested treatment regimens on male rats first and

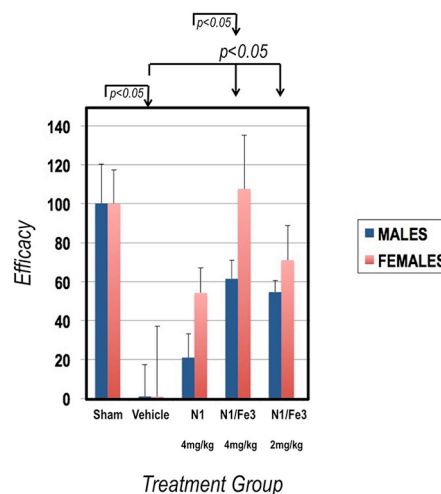


**Figure 1.** Aggregate efficacy plot for selected treatment regimens in both sexes, with sham group set to 100 and vehicle group set to 1 for each sex.

confirmed the efficacy of the most informative treatment regimens on female rats. We did not observe effects in two of the seven classes (hyper-angiogenesis, weight loss), possibly because the modified scald for female rats was milder. Thus, aggregate efficacy computations for male rats averaged seven efficacy classes and for female rats, five classes. A comparison aggregate efficacy plot for both sexes is shown in Figure 1.

### Male rats: ferric iron improves efficacy of nephrlin peptide

Table 1 shows the results obtained when male rats in the scald model were exposed to vehicle, 4 mg/kg nephrlin and 4 mg/kg nephrlin complexed with either ferric iron, ferrous iron or zinc. To make global comparisons of treatment efficacy, we converted values to z-scores. All scores within an efficacy class were averaged, allowing allocation of equal weight to efficacy classes. A composite z-score (average z score across all seven effect classes) is shown in the last row of the table. This allows direct comparison of efficacy across treatment groups. The sham treatment involves manipulating the animals exactly as in the burn group, but without the burn treatment. The efficacy value for the sham (0.82) is thus the positive control. The negative control is the Burn + vehicle group (-0.61). The results show that ferric iron supplementation is superior to the other metals (efficacy of 0.27 vs. 0.01 and -0.19 for zinc and ferrous iron, respectively) in improving the efficacy of nephrlin on the following clinically relevant readouts: early hyperinflammation (24-h

plasma IL-6), inflammasome activation at two weeks (IL-18, IL-1-beta), hyperangiogenesis (VEGF-A, CCL5, CXCL5, PctRedPix), glycaemic control, kidney function, oxidative stress and weight loss. Compared to vehicle or nephrilin treatment alone (-0.31), nephrilin with ferric iron (0.27) is at least twice as efficacious overall.

### *Male rats: dose ranging of nephrilin-ferric iron treatment*

Table 1 shows the results obtained when male rats in the scald model were exposed to vehicle, 2, 4 and 8 mg/kg nephrilin complexed with ferric iron. The results show that 2 mg/kg (0.17) and 4 mg/kg (0.27) dose levels were superior to 8 mg/kg (-0.37). This surprising result may indicate that, at high doses, the pool of 'free' iron in equilibrium may reach detrimental levels.

### *Female rats: nephrilin in female rats shows improved efficacy with ferric iron*

Table 2 shows the results obtained when female rats in the scald model were exposed to vehicle or nephrilin complexed with ferric iron. As in male rats, ferric iron increased the potency of 4 mg/kg nephrilin (2.45 vs. 0.48) in the presence of ferric iron. This result confirms the effect of ferric iron seen in male animals.

### *A similar pattern of improvement is seen with ferric iron supplementation in both sexes*

Figure 1 shows a composite of the efficacies computed for key treatments in both sexes. A similar pattern of efficacy is seen for ferric iron supplementation in the dose range of 2–4 mg/kg for both sexes.

## **Discussion**

In rodent models of stress, nephrilin peptide has been shown to reverse elevations in neuroimmune and oxidative stress consequent to thermal, metabolic and xenobiotic insult.<sup>14,15,18,19</sup> Dysregulated host immune responses to traumatic stress, massive infection and other severe challenges sometimes exhibit a time-course of hyperinflammation—often leading to multiple organ failure, sepsis or death—followed by chronic critical illness, recently dubbed Persistent Inflammation, Immunosuppression and Catabolism Syndrome (PICS).<sup>22,25</sup> PICS

represents an alarming and rapidly expanding burden on the healthcare system. Nephrilin's efficacy in reversing the systemic effects of sepsis and burn trauma, including loss of glycaemic control, body mass, kidney function, wound healing capacity and sepsis<sup>14,15,18</sup> appears to involve this pleiotropic dysfunction.

In recent years, our understanding of PICS has evolved. Readouts such as elevated plasma IL-6 at 24 h post-insult, chronic inflammasome activation, loss of body mass, wound healing impaired by excessive angiogenesis, loss of glycaemic control, elevated markers of oxidative stress, immune dysregulation and neurodegenerative consequences, among others, have emerged as emblematic of the progression of PICS.<sup>22–27</sup>

In a previous study,<sup>15</sup> the possible effect of iron in the efficacy of nephrilin peptide in a rat scald model was suggested. Here we show that, in both sexes of rats, the addition of equimolar ferric iron (but not ferrous iron or zinc) roughly doubles the efficacy of the peptide in the model. However, the optimal dose range for the dosing regimen adopted (subcutaneous bolus injection, once daily, for seven days after burn) appears to be 2–4 mg/kg/day. At a higher dose (8 mg/kg/day), a reduced efficacy was observed. One possible explanation for the lowered efficacy observed at high doses of nephrilin-ferric-iron (N1/Fe3) formulations is that the 'free' pool of iron expected to equilibrate into circulation has some negative effect, such as increasing oxidative stress. In support of this hypothesis, elevated plasma OHDG levels were not reduced at the higher dose.

NLRP3 inflammasome activation in burn injury appears to be a double-edged sword: a small amount may be helpful to healing, but excessive activation is associated with poor outcomes.<sup>23</sup> We showed that N1/Fe3 treatments significantly reduced plasma levels of IL-18 and IL-1-beta, markers of NLRP3 inflammasome activation. Similarly, although angiogenesis is beneficial to early stages of wound healing, pathological angiogenesis may reduce capacity for complete wound healing.<sup>24</sup> Our readouts of pathological angiogenesis included VEGF-A, CCL5, CXCL5 and a visual measure of percent red pixels in wounds, PctRedPix. N1/Fe3 treatments at 2–4 mg/kg significantly reduced readouts in this class. To our knowledge, this is the first demonstration of the use of this class of readouts in a burn model.

The present study confirmed each of our earlier findings regarding the robust effects of nephrilin peptide on early IL-6 elevation, and other

**Table 1.** Efficacy in male rats.

Effect class	S (Sham)	B (vehicle)	N1 (4 mg/kg)	N1/Zn2 (4 mg/kg)	N1/Fe2 (4 mg/kg)	N1/Fe3 (2 mg/kg)	N1/Fe3 (4 mg/kg)	N1/Fe3 (8 mg/kg)
1	31.4 ± 12.0*	62.3 ± 16.9	50.6 ± 6.1	43.4 ± 13.6*	49.1 ± 13.1	38.5 ± 27.8	41.4 ± 11.2*	48.5 ± 18.5
2a	125.2 ± 45.5*	203.8 ± 61.8	178.1 ± 19.3	133.3 ± 25.1	157.7 ± 70.7	220.4 ± 32.1	119.1 ± 15.4*	148.2 ± 61.7
2b	41.9 ± 12.3*	266.8 ± 185.2	124.3 ± 132	36.7 ± 9.5*	97.4 ± 86.6	52.9 ± 7.8*	36.6 ± 7.8*	254.5 ± 291.9
3a	50.4 ± 10.2*	67.4 ± 17.4	56.1 ± 11.7	38.3 ± 8.8*	41.2 ± 6.8*	37.8 ± 15.3*	48.1 ± 10.9*	43.3 ± 8.1*
3b	218.1 ± 41.8*	664.8 ± 42.8	609.7 ± 283	321.1 ± 96	249.8 ± 73*	248.3 ± 29.7*	192.1 ± 26.3**	301.2 ± 74.9
3c	763 ± 229*	2009 ± 745	1910 ± 380	1154 ± 224*	939 ± 300†	855 ± 233**	1038 ± 495*	1435 ± 445
3d	n/a	20.01 ± 1.37	16.51 ± 3.02	9.74 ± 5.79*	11.79 ± 5.6*	6.53 ± 3.16*	8.65 ± 3.35**	18.3 ± 11.83
4	78.4 ± 43.4*	157.3 ± 69.8	139.3 ± 48.6	215.6 ± 124	120.6 ± 65.4	136.4 ± 69.2	94.3 ± 25.4*	93.8 ± 37.2*
5	0.23 ± 0.03*	0.38 ± 0.18	0.34 ± 0.13	0.26 ± 0.12	0.38 ± 0.16	0.31 ± 0.09	0.18 ± 0.11**	0.38 ± 0.12
6	479 ± 116*	665 ± 78	585 ± 137	454 ± 76†	455 ± 71†	374 ± 187**	423 ± 79**	761 ± 89
7	5.58 ± 1.00*	2.34 ± 1.03	2.32 ± 1.01	1.66 ± 1.08	2.65 ± 0.56	2.99 ± 0.53	2.71 ± 1.62	2.50 ± 0.55
Average	0.82 ± 0.58*	-0.61 ± 0.47	-0.31 ± 0.35	0.01 ± 0.62*	-0.19 ± 0.52*	0.17 ± 0.40*	0.27 ± 0.60**	-0.37 ± 0.45

Treatment groups (n=8) are described in the 'Materials and methods' section.

Effect classes: 1 = early inflammation (24h plasma IL-6 pg/mL); 2 = 14-day plasma inflammation markers (2a = IL18 pg/mL; 2b = IL1b pg/mL); 3 = 14-day plasma hyperangiogenesis markers (3a = VEGF-A pg/mL; 3b = CCL5 pg/mL; 3c = CXCL5 pg/mL; 3d = PctRedPix); 4 = glycaemic control, 14-day GTT (AUC mg.dL.h); 5 = kidney function, 14-day plasma (creatinine mg/dL); 6 = systemic oxidative stress, 14-day plasma (OHDG pg/mL); 7 = weight loss (slope).

\* $P < 0.05$  vs. B group.

† $P < 0.05$  vs. N1 group.

‡ $P < 0.05$  vs. 8 mg/kg group.

**Table 2.** Efficacy in female rats.

Effect class	S (Sham)	B (vehicle)	N1 (4 mg/kg)	N1/Fe3 (2 mg/kg)	N1/Fe3 (4 mg/kg)
1	46 ± 13	63 ± 15	51 ± 9	51 ± 12	36 ± 15*
2	129.6 ± 24.1*	170.4 ± 28.8	154.1 ± 30.3	155.2 ± 39.9	137.0 ± 19.4*
4	55.9 ± 17.9*	95.1 ± 40.3	67.5 ± 19.8	79.2 ± 21.7	52.3 ± 19.2*†
5	0.26 ± 0.02*	0.31 ± 0.03	0.24 ± 0.04*	0.22 ± 0.07*	0.26 ± 0.03*
6	216 ± 116*	765 ± 152	633 ± 263	363 ± 251*	452 ± 147*
Average	2.17 ± 1.27*	-1.52 ± 2.67	0.48 ± 0.96	1.10 ± 1.31	2.45 ± 2.04*

Treatment groups (n=8) are described in the 'Materials and methods' section.

Effect classes: 1 = early inflammation (24-h plasma IL-6 pg/mL); 2 = 14-day plasma inflammasome marker IL18 pg/mL; 4 = glycaemic control, 14-day GTT (AUC mg.dL.h); 5 = kidney function, 14-day plasma (creatinine mg/dL); 6 = systemic oxidative stress, 14-day plasma (OHDG pg/mL).

\* $P < 0.05$  vs. B group.

† $P < 0.05$  vs. N1 group.

clinically relevant effects on glycaemic control, kidney function, loss of body mass and systemic oxidative stress in the rat scald model.<sup>8,14,15</sup> The present study further showed efficacy of nephrlin for both sexes in most of these effect classes. This is the first time that the efficacy of nephrlin in this model has been tested in female rats. Perhaps because of anatomical differences (which affect scald exposure) and possible confounding influences of the oestrous cycle, female rats have rarely been investigated in this type of rat scald model. Our results suggest that the improved efficacy of treatments with nephrlin-iron versus nephrlin alone were similar in both sexes.

Our results also raise obvious questions for future study. Is it possible to modify the iron-binding properties of this peptide so as to allow for tighter binding of the metal and possibly higher dose efficacy? Can this peptide be coupled to other moieties to improve effective treatment of burn trauma? We intend to address these questions in future experiments.

### Declaration of conflicting interests

The author(s) declared no potential conflicts of interest with respect to the research, authorship, and/or publication of this article.

### Funding

The author(s) disclosed receipt of the following financial support for the research, authorship, and/or publication of this article: This project was supported by the following grants: 1R43GM131424 to DDM.

### ORCID iD

Desmond D Mascarenhas  <https://orcid.org/0000-0002-0710-9960>

### References

- Jacinto E, Loewith R, Schmidt A, et al. Mammalian TOR complex 2 controls the actin cytoskeleton and is rapamycin insensitive. *Nat Cell Biol* 2004; 6: 1122–1128.
- Facchinetti V, Ouyang W, Wei H, et al. The mammalian target of rapamycin complex 2 controls folding and stability of Akt and protein kinase C. *EMBO J* 2008; 27: 1932–1943.
- Garcia-Martinez JM and Alessi DR. mTOR complex 2 (mTORC2) controls hydrophobic motif phosphorylation and activation of serum- and glucocorticoid-induced protein kinase 1 (SGK1). *Biochem J* 2008; 416: 375–385.
- Singh BK, Singh A and Mascarenhas DD. A nuclear complex of rictor and insulin receptor substrate-2 is associated with albuminuria in diabetic mice. *Metab Syndr Relat Disord* 2010; 8: 355–363.
- Singh B, Charkowicz D and Mascarenhas D. Insulin-like growth factor-independent effects mediated by a C-terminal metal-binding domain of insulin-like growth factor binding protein-3. *J Biol Chem* 2004; 279: 477–487.
- Huq A, Singh B, Meeker T, et al. The metal-binding domain of IGFBP-3 selectively delivers therapeutic molecules into cancer cells. *Anticancer Drugs* 2009; 20: 21–31.
- Morrison MM, Young CD, Wang S, et al. mTOR Directs Breast Morphogenesis through the PKC-alpha-Rac1 Signaling Axis. *PLoS Genet* 2015; 11: e1005291.
- Mascarenhas DD, Herndon DN and Arany I. Epigenetic Memory of Oxidative Stress: Does Nephrlin Exert Its Protective Effects Via Rac1? *Biologics* 2017; 11: 97–106.
- Jeschke MG, Pinto R, Kraft R, et al. Morbidity and survival probability in burn patients in modern burn care. *Crit Care Med* 2015; 43: 808–815.
- Jeschke MG, Pinto R, Herndon DN, et al. Hypoglycemia is associated with increased postburn morbidity and mortality in pediatric patients. *Crit Care Med* 2014; 42: 1221–1231.

11. Chondronikola M, Meyer WJ, Sidossis LS, et al. Predictors of insulin resistance in pediatric burn injury survivors 24 to 36 months postburn. *J Burn Care Res* 2014; 35: 409–415.
12. Patel P, Sallam HS, Ali A, et al. Changes in fat distribution in children following severe burn injury. *Metab Syndr Relat Disord* 2014; 12: 523–526.
13. Kraft R, Herndon DN, Finnerty CC, et al. Occurrence of multiorgan dysfunction in pediatric burn patients: incidence and clinical outcome. *Ann Surg* 2014; 259: 381–387.
14. Mascarenhas DD, Elayadi A, Singh BK, et al. Nephrlin peptide modulates a neuroimmune stress response in rodent models of burn trauma and sepsis. *Int J Burns Trauma* 2013; 3: 190–200.
15. Mascarenhas DD, Ayadi AE, Wetzel M, et al. Effects of the nephrlin peptide on post-burn glycemic control, renal function, fat and lean body mass, and wound healing. *Int J Burns Trauma* 2016; 6: 44–50.
16. Sihler KC, Raghavendran K, Westerman M, et al. Hepcidin in trauma: linking injury, inflammation, and anemia. *J Trauma* 2010; 69: 831–837.
17. Herndon DN, Wilmore DW and Mason AD, Jr. Development and analysis of a small animal model simulating the human postburn hypermetabolic response. *J Surg Res* 1978; 25: 394–403.
18. Mascarenhas D, Routt S and Singh BK. Mammalian target of rapamycin complex 2 regulates inflammatory response to stress. *Inflamm Res* 2012; 61: 1395–1404.
19. Conrad ME and Umbreit JN. Pathways of iron absorption. *Blood Cells Mol Dis* 2002; 29: 336–355.
20. Huq A, Singh B, Meeker T, et al. The metal-binding domain of IGFBP-3 selectively delivers therapeutic molecules into cancer cells. *Anticancer Drugs* 2009; 20: 21–31.
21. Fleck C. Determination of the glomerular filtration rate (GFR): methodological problems, age-dependence, consequences of various surgical interventions, and the influence of different drugs and toxic substances. *Physiol Res* 1999; 48: 267–279.
22. Hawkins RB, Raymond SL, Stortz JA, et al. Chronic Critical Illness and the Persistent Inflammation, Immunosuppression, and Catabolism Syndrome. *Front Immunol* 2018; 9: 1511.
23. Vinaik R, Stanojic M and Jeschke MG. NLRP3 Inflammasome Modulates Post-Burn Lipolysis and Hepatic Fat Infiltration via Fatty Acid Synthase. *Sci Rep* 2018; 8: 15197.
24. Ridiandries A, Tan JT, Ravindran D, et al. CC-chemokine class inhibition attenuates pathological angiogenesis while preserving physiological angiogenesis. *FASEB J* 2017; 31: 1179–1192.
25. Qiao Z, Wang W, Yin L, et al. Using IL-6 concentrations in the first 24 h following trauma to predict immunological complications and mortality in trauma patients: a meta-analysis. *Eur J Trauma Emerg Surg* 2018; 44: 679–687.
26. Jeschke MG. Clinical review: Glucose control in severely burned patients - current best practice. *Crit Care* 2013; 17: 232.
27. Purohit M, Goldstein R, Nadler D, et al. Cognition in patients with burn injury in the inpatient rehabilitation population. *Arch Phys Med Rehabil* 2014; 95: 1342–1349. <https://www.ncbi.nlm.nih.gov/pubmed/24582616>

### How to cite this article

Mascarenhas DD, El Ayadi A, Ravikumar P, Kang GJ, Langer T, Moreno C and Amento EP. Positive effects of ferric iron on the systemic efficacy of nephrlin peptide in burn trauma. *Scars, Burns & Healing*, Volume 6, 2020. DOI: 10.1177/2059513118928494.